NUMERICAL AND EXPERIMENTAL INVESTIGATION OF THE OPERATING CHARACTERISTICS OF A LONG 'WICKED' HEAT PIPE

S. B. Riffat, X. Zhao, P. S. Doherty
School of the Built Environment, The University of Nottingham,Nottingham, NG7 2RD, UK
Tel: +44-115-951 3157; Fax: +44-115-951 3159, Email: saffa.riffat@nottingham.ac..uk

Song Lin
Thermacore Europe Ltd, Unit 12 Wansbeck Business park, Ashington, Northumberland, NE63 8QW, UK
Tel: +44-1670 859 525; Fax: +44 1670 859 539, Email: Song.lin@thermacore.com

Abstract

In this paper, a simplified numerical model was developed based on the analysis of previous modeling methods. Investigation of the operating characteristics of a long 'wicked' heat pipe was carried out numerically and experimentally. Finite-difference method was employed to carry out numerical analysis, and FORTRAN language was used to develop a computer program. Mathematical theories and numerical method used for this analysis were discussed. A test rig was constructed to carry out lab testing. The liquid and vapour flows, pressures and temperature in different areas of the heat pipe were simulated and the results were indicated as the function of the height above the filled liquid level as well as the radius in relative to the central line of the pipe. Lab testing was conducted to measure the temperature and heat flow associated with the heat pipe heat transfer. Comparison of numerical predictions and testing results was carried out. It is found that the results from tests are in good agreement with the numerical predictions when the test conditions are close to the simulation assumption. This demonstrates that the numerical model is able to provide a reasonable accuracy for predicting the operating characteristics of the heat pipe.

KEYWORDS

Heat Pipes; Wicks; Numerical; Experiment; Investigation.

INTRODUCTION

Over the past 30 years, extensive studies have been conducted in order to provide a through understanding of the heat pipe operation and appropriate design schemes for practical applications. As a result, numerous methods, covering a variety of aspects of heat pipe operations, have been developed [1]. Experimental studies were also conducted to provide useful insights into heat pipe operations, set references for validation of theoretical models, and provide databases for design purposes. In addition, many theoretical analyses have incorporated empirical or semi-empirical correlation to simplify the models and the solution process.

The complicated mathematical expressions and numerical schemes in the previous studies were helpful, but sometimes may 'mask' the real physics from a designer's point of view. For most practical applications, it is usually not desirable or necessary to get into such details. Therefore, a simple and practicable model for the heat pipe analysis may be more attractive.

NUMERICAL MODEL SET-UP - MATHEMATICAL THEORY AND NUMERICAL METHOD

A numerical model was developed based on the analysis of the previous methods. The model allows some assumptions to be made for simplification, but is still able to provide a reasonable accuracy for practical application. In this model, vapour flow in the simulated heat pipe (8mm diameter) is treated as a two-dimensional problem. This is because the vapour cross-sectional area

is relatively large, which would result in a remarkable variation of vapour parameters along the radial direction. Heat transfers through liquid-wick and wall regions are computed by solving a one-dimensional heat conduction equation. This is rational because of the following two reasons: First, the heat transfer in a heat pipe is mainly conducted by evaporation and condensation of vapour flow, and secondly, heat input across the evaporator area and heat output across condenser area are evenly distributed, which result in an even temperature distribution around the evaporator and condenser areas. As a result, heat conduction through wall and liquid-wick region is mainly directed toward radial direction, rather than axial direction. Flow in the liquid region was treated as a one-dimensional problem. This is because the liquid in a heat pipe was evenly distributed around the periphery of heat pipe inner wall, which would form a very thin liquid film over the wicked area. The film was so thin (about 0.1mm) that the variation of liquid parameters across the film could be negligible.

Liquid and vapour flows are jointly analysed by using a set of governing equations. To make the joint analysis more easy and simple, the vapour flow was initially treated as a one-dimensional flow. Solving the one-dimensional model would obtain the first set of results. The results obtained are then used to activate a two-dimensional vapour flow model. This would give another set of results, including vapour flow parameters within the heat pipe space, as well as refined vapour pressure gradient. The values of pressure gradient from two solution processes are compared, and the error for the pressure gradient is obtained. If the error is larger than 5%, then the iteration for the selected element (section) continues by replacing the first value of pressure gradient with the second one. Otherwise, the iteration for the selected element terminated and the iteration for the next selected element started. Finite-difference method was employed to carry out numerical analysis for the equation solutions, and the FORTRAN language was used to develop a computer program.

Mathematical Theory

As indicated above, vapour flow in the simulated heat pipe was initially treated as a one-dimensional flow. The flow could be analysed by coupling the governing equations with those of liquid flow, and of heat conduction for the heat transfer across wall and liquid-wick regions.

The high thermal conductivity of heat pipes is the result of the continued evaporation and condensation process occurring within the heat pipe. For this reason, the determination of evaporation and condensation rates plays a key role in evaluating heat pipe operating characteristics. In this model, an expression for the free molecular flow mass flux of evaporation, j, presented by Collier [2] and later used by Colwell and Chang [3], was employed:

$$j = [\frac{M}{2\pi R(t+273)}]^{0.5}(\pi_\sigma - \pi_v)\,. \tag{1}$$

When p_s is greater than p_v, j is positive and the liquid evaporated. When p_s is less than p_v, j is negative and the vapour condensed. In the development of the numerical model, the evaporation-condensation rate is assumed to be proportional to the liquid-vapour interface area in each section of the heat pipe, i.e.,

$$\Delta m_{ec} = jW_{ec}\Delta x\,. \tag{2}$$

For a given latent heat, h_{fg}, the rate of heat removed or absorbed in any section can be determined from:

$$q_{ec} = h_{fg}\Delta m_{ec}\,. \tag{3}$$

For a wicked heat pipe to operate properly, the capillary pressure difference, plus gravity difference, must be sufficient to overcome the liquid and vapour pressure losses. However, for a wickless heat pipe to operate properly, gravity difference is the sole force used to overcome the liquid and vapour pressure losses.

Capillary pressure is expressed as

$$p_{cl} = 2s\ \cos q / r_{ce}\,. \tag{4}$$

Since both p_{cl} and r_{ce} are functions of length position x, then

$$\frac{dp_{cl}}{dx} = \frac{-2s\ \cos q}{r_{ce}^{\,2}} \frac{dr_{ce}}{dx}\ . \tag{5}$$

Expressing this over a finite interval yields:

$$\Delta p_{cl} = (-2s\ \cos q / r_{ce}^{\,2})\Delta r_{ce}\ . \tag{6}$$

Gravity pressure differences include axial and radial pressure differences. They are expressed respectively as follows:

$$\Delta \mathrm{p}_{\mathrm{ag}} = -\rho_{\mathrm{l}} \mathrm{g} \sin\phi \Delta \mathrm{x}\,, \tag{7}$$

$$\Delta \mathrm{p}_{\mathrm{rg}} = -2\rho_{\mathrm{l}} \mathrm{g} \cos\phi \Delta \mathrm{r}_{\mathrm{v}}\,. \tag{8}$$

The pressure losses of liquid and vapour are expressed as

$$\Delta p_{vl} = \Delta p_{fv} + \Delta p_{mv} + \Delta p_{fl} + \Delta p_{ml}\,. \tag{9}$$

The pressure losses result from liquid and vapour friction, and the momentum changes occurring in any one section along the heat pipe. The pressure losses due to friction for laminar flow may be expressed as:

$$\Delta p_{fv} = (2m_v \Delta x u_{v)/ r_{hv}}^{\,2}, \tag{10}$$

$$\Delta p_{fl} = (2m_l \Delta x u_l) / r_{hl}^{\,2}. \tag{11}$$

The total pressure drop due to the momentum change may be expressed as:

$$\Delta p_{ml} = (u_l \Delta m s_l + m s_l \Delta u_l + \Delta m s_l \Delta u_l) / A_l\,, \tag{12}$$

$$\Delta p_{mv} = (u_v \Delta m s_v + m s_v \Delta u_v + \Delta m s_v \Delta u_v) / A_v\,. \tag{13}$$

For steady state model the energy equation may be written as:

$$q_{in} = q_{out}\,, \tag{14}$$

$$q_{in} = m s_0 h_{fgv0} + m s_1 h_{fgl1} + q\ , \tag{15}$$

$$q_{out} = m s_1 h_{fgv1} + m s_0 h_{fgl0}\,, \tag{16}$$

$$q = q_{ec}\,. \tag{17}$$

The continuity equation may be written as:

$$\int r_v A_v dx + \int r_l A_l dx = cons\tan t\ . \tag{18}$$

Both the wicked and wickless heat pipes consist of two (or three) basic sections, i.e., the evaporation section, the adiabatic section and the condensation section. Each section has a different set of boundary conditions, and as a result, needs to be treated independently.

Following the simplified one-dimensional mathematical analysis, the vapour flow is further analysed by using a two-dimensional theory. The analysis is started by using the results obtained from the initial analysis. The vapour flow could be assumed as a steady, incompressible, axisymmetric (for circular

pipes) and laminar flow for simplification [4]. The radial velocity through liquid-vapour interface is a constant either in the evaporation section or in the condensation section. The variation of pressure occurs along the axial direction rather than the radial direction. The equations governing laminar vapour flow in a circular heat pipe are:

Axial momentum equation: $$u\frac{\partial u}{\partial x}+v\frac{\partial u}{\partial r}=\frac{-1}{r}\frac{dp}{dx}+\nu(\frac{\partial^2 u}{\partial r^2}+\frac{1}{r}\frac{\partial u}{\partial r}). \quad (19)$$

Continuity equation: $$\frac{\partial u}{\partial x}+\frac{1}{r}\frac{\partial(vr)}{\partial r}=0. \quad (20)$$

The boundary conditions are
$u(0, r) = c_0$; $u(1, r) = 0$; $v(0, r) = v(1, r) = 0$; $v(x, 0) = 0$; $\partial u/\partial r\ (x,0) = 0$; $u(x, r_0) = 0$; $v(x, r_0) = c$.

Where c is a constant and in the evaporation section, $c > 0$ (injection); in adiabatic section, $c = 0$; and in the condensation section, $c < 0$ (suction). Of which (a) and (b) are end wall conditions, (c) and (d) are axial conditions, (e) is the non-slip condition and (f) is side wall condition.

Numerical Method

The finite-difference scheme is initially used to carry out numerical analysis and solution solving for the one-dimensional vapour flow model. In the initial analysis, both vapour and liquid are treated as one-dimensional flows, and the flow parameters vary only along the axial direction. The governing equations are applied to sections, grids and control volumes in a sequence order, which start from the control points and surfaces on the interface of liquid and vapour, and the boundary of liquid and wall. The trial-and-error method is employed and the error limit is set to 5% for this simulation. The subsequent analysis is based on a two-dimensional vapour flow model. In this analysis, the grid distribution and mesh network are slightly different from that of a one-dimensional assumption.Given a section of heat pipe along the flow as the simulated element, vapour is initially treated as a one-dimensional flow, and the governing equations are coupled with those of liquid flow, as well as those for heat conduction through liquid and wall regions. Solving the correlated equations will give a set of results, including liquid flow parameters (u_l, p_l, a_l etc), geometrical parameters of the interface of liquid and vapour phases(r_v etc), as well as pressure gradients of liquid and vapour phases (Δp_l and Δp_v).

The results obtained are then used to activate a two-dimensional vapour flow model, which acts as the replacement of the one-dimensional one. This will give another set of results, including vapour flow parameters within the heat pipe space (u_v and v_v), as well as refined vapour pressure gradient (Δp_v'). The values of Δp_v and Δp_v' are compared, and the term of (Δp_v'-Δp_v)/ Δp_v' is defined as the calculation error, p_e. If the absolute value of p_e is larger than 5%, then the iteration in this element continues by replacing Δp_v with Δp_v'. Otherwise, the iteration in this element is terminated and the iteration in the next element starts.

Modelling results of the Selected Heat Pipe

A 1.97m long heat pipes was selected as the simulated object. The pipe was fitted with two wraps of copper screen meshes on its inner surface, which is called wicks. The design parameters were determined and the simulation conditions were assumed, as detailed in Table 1. The analysis calculation showed that the maximum heat transport capacity of the wicked pipe is 314W. Numerical analysis was conducted to evaluate the operating characteristics of the heat pipes, as indicated below.

Variation of liquid and vapour flows

Variation of average vapour and liquid velocities with hight position above the filled liquid level was simulated. In the condensation section, vapour velocity decreases along the flow direction (upward), and liquid velocity increases along the flow direction (downward), due to a dramatic condensation. Even so, liquid cross-sectional area still increases along the liquid flow direction (downward), resulting in the decrease of vapour cross-sectional area. This is because liquid flow is not fast enough to remove condensed liquid promptly. In the adiabatic section, liquid and vapour cross-sectional areas, as well as

flow velocities, remain the constant along the flow direction. This is because no heat transfer occurs in this area due to a good insulation provided. In the evaporation section, vapour and liquid flows behaviours in contrast with that in the condensation section. On the interface of the evaporation section and the adiabatic section, liquid volume achieves its maximum value, resulting in the maximum liquid cross-sectional area and the minimum vapour cross-sectional area. Along the liquid flow direction (downward), some of the liquid absorbs heat striking on the heat pipe outer surface and is vaporized, and the other keeps the flow trend along the pipe inner wall. The velocity of liquid flow, as well as the liquid cross-sectional area, decreases along its flow direction (downward), due to the decrease of liquid volume. Consequently, vapour cross-sectional area decreases along the flow direction (upward).

Variation of axial vapour velocities with height position above the filled liquid level for the wicked pipe was simulated. In the same cross section, the axial velocity appears to be higher in the central area, and lower in the boundary area. The variation of the velocity across radial direction shows a parabolic shape. Along the height position, the axial velocity increases slightly in the evaporation section, remains the same in the adiatic section, and decreases significantly in the condensation section due to a relatively shorter condensing distance.

Variation of radial vapour velocity along radial direction at different height positions (above the filled liquid level) was indicated. In the evaporation section, The radial flow velocity is negative and its absolute value decreases gradually from the periphery to the centre area, which means an inward flow existed due to a constant injection from the interface of liquid/vapour phases. In the adiabatic section, The radial flow velocity is zero, which means no radial flow existed due to absence of injection/ejection on the interface of liquid/vapour phases. However, in the condensation section, the radial velocity becomes postive and its absolute value increases gradually from the central area to the periphery, which means an outward flow existed due to a constant ejection from the interface of the liquid/vapour phases.

Variation of vapour, liquid and inner wall pressures

Relationship of liquid, vapour and inner wall pressures with height position for the wicked heat pipe was indicated. In the evaporation section, inner wall pressure is higher than vapour pressure, which results in liquid vaporization. However, in the condensation section, inner wall pressure is lower than vapour pressure, which results in vapour condensation. Liquid pressure is much lower than vapour and inner wall pressures as part of its static pressure is converted into velocity pressure, causing the fluid flow within the heat pipe.

Variation of temperatures

Variations of the temperatures of vapour, liquid, wall, heat/cool sources and heat conduction/convection mediums with height position for the wicked pipe was simulated. There are very little differences among vapour, liquid and wall temperatures, compared to the differences of vapour (liquid or wall) and heat/cool sources and heat conduction/convection mediums. This demonstrates that the heat pipe is an excellent heat transfer device, and operated at an approximately constant temperature. The major heat resistances occur in the heat conduction/convection mediums, which result in significant variation of temperature within these areas. For this case, the heat conduction/convection mediums are the still air filled into the heating element vessel in the evaporation section, and the cooling water circulated through water jacket in the condensation section.

Experimental testing of the selected heat pipes

A rig was constructed to test the operating characteristics of the wicked heat pipe [5]. A picture showing the real view is presented in Figure 1. A flexible heating element was wrapped along the evaporation section, which allowed a gap existed between the heat pipe outer-surface and the heating element inner-surface in order to create an identical heat input over the evaporator area. Insulation was covered outside the heating element to reduce heat loss to environment. The value of the heating element output was controlled by a Variac. The condensation section of the heat pipe was inserted into a water-cooled jacket, which was connected to a cooling water loop. An air cooler was used to remove heat away from the heat pipe, and a pump used to run the circulation. A single jet water meter was assembled to measure the water flow rate, by giving the overall flow volume and time duration of the testing. Two valves were installed to adjust water flow rate and jacket inlet/outlet temperatures. In this testing, adjusting was purposely made to keep the average temperature of jacket water same as the

assumed in the numerical simulation, to enable the comparison between the numerical predictions and the testing results.

T-type thermocouples were mounted to measure the temperatures of a few points on the heat pipe outer surface, as well as those at the jacket inlet and outlet. Windmill, the data logger system was used to acquire the data. The energy balance test was carried out to validate the test rig.

Similar tests were carried out for three times using the rig, in order to validate the reliability of the measurement data. Each test took about 2 hours. It was found that the steady state was achieved about 30 minutes after starting-up. The test results at the steady state were recorded, which are detailed in Table 2.

It should be mentioned that although the thermocouples were sticking onto the outer surface of the heat pipe either in the evaporation section or in the condensations section, they still not give the real values of the surface temperatures. The reason for this is the thermocouples not only touch the outer surface of the heat pipe, but also were exposed to surrounding mediums, such as hot air between the heating element and the outer surface of the heat pipe (evaporation section), and the inner surface of the cooling jacket (condensation section). In fact, the thermocouples give the mixture feeling for the heat pipe outer surface and surroundings. Therefore, the measurement data should be values that are between outer surface temperature and surrounding temperature.

Comparison of Numerical Predictions and Testing Results

Comparisons between numerical predictions and testing results were made, as shown in Figures 2. The results from tests 1 & 2 are in good agreement with numerical prediction as the test conditions are very close to the simulation assumptions. However, results from test 3 are away from the numerical predictions, as the test conditions are bitter different from the simulation assumptions.

The Figure 2 displayed the data measured from the thermocouples on the outer surface of the heat pipe, as well as the numerical temperature values of outer surface, surrounding fluids (heat transfer fluids) and heat/cooling sources. It is found that the data given by the thermocouples were between heat pipe outer surface temperatures and surrounding temperatures, a little close to the surface temperatures.

This testing was constrained to temperature item due to difficulty of testing any other parameters (pressure, velocity, flow distribution) for heat pipe operation using the rig above. Therefore, further comparison among numerical prediction and experimental results becomes unavailable. However, comparison for temperature item has already demonstrated that the numerical model is able to give a reasonable accuracy for predicting operating characteristics of the wicked heat pipe.

CONCLUSIONS

A simplified numerical model was developed based on the analysis of the previous methods, and this was used to investigate the operating characteristics of the selected heat pipe. Lab testing was carried out to investigate its operating characteristics as well. Comparisons between numerical predictions and testing results were carried out. It is found that the results from tests are in good agreement with numerical prediction when the test conditions are close to the simulation assumption. Although tests were constrained to temperature item due to difficulty for testing of any other parameters, which made further comparison unavailable, the current comparison for temperature item has already validate the availability of the numerical model.

Nomenclature

A-cross-sectional area (m^2)
θ-wetting angle of liquid-vapor surface (deg)
d-diameter (m)
h_{fg}-latent heat of vaporization (J/kg)
ρ-density (kg/m^3)
σ-surface tension (N/m)

R-universal gas constant, 8317 (J/kg.K)
g-gravitational acceleration (m/s^2)
ϕ-angle of inclination relative to horizontal surface (deg)
q_c-heat input (W)
T-absolute temperature (K)
t-temperature (^oC)
P-pressure (Pa)
P_{cl}-capillary pressure (Pa)
Δp_{cl}-net capillary pressure difference (Pa)
Δp_l-viscous pressure drop occurring in the liquid phase (Pa)
Δp_v-viscous pressure drop occurring in the vapour phase (Pa)
Δti-time interval used in the iteration (second)
Δt -temperature increase during the time interval (^oC)
C_p -specific heat of liquid (kJ/kg.K)
μ dynamic viscosity ($N.s/m^2$)
ν-velocity viscocity (m^2/s)
W_{ec}-perimeter of the vapour-liquid interface (m)
j-free molecular flow mass flux of evaporation ($kg/m^2.s$)
M-molecular weight
q_{ec}-heat transfer rate on the vapour-liquid interface in the element (W)
Δq-heat increase in an element unit at ΔT time interval in transient state (W)
Δm_{ec}-evaporation-condensation rate in the liquid-vapour interface of the element (kg/s)
Δp_{rg}-radial hydrostatic pressure difference (Pa)
Δp_{ag}-axial hydrostatic pressure difference (Pa)
Δp_{vl}-difference of the vapour and liquid pressure in the element (Pa)
Δp_{fv}-friction pressure loss occurring in the vapour phase (Pa)
Δp_{mv}-pressure loss due to momentum change occurring in the vapour phase (Pa)
Δp_{fl}-friction pressure loss occurring in the liquid phase (Pa)
Δp_{ml}-pressure loss due to momentum change occurring in the liquid phase (Pa)
u-axial velocity (m/s)
Δu-axial velocity difference between the two sections of the element (m/s)
v-radial velocity (m/s)
Δv-axial velocity difference between the two sections of the element (m/s)
Δms-difference of mass flow rates between the two sections of the element (kg/s)
ms-average mass flow rate in the element (kg/s)

Subscripts

v-vapour
l-liquid
s-solid
0 inlet of the element
1 outlet of the element

Table 1. Design parameters and simulation conditions

Quantities	Values
Dimension	1970 (mm length) × 8 (mm outer diameter)
Evaporating section	1700 mm
Adiabatic section	70 mm
Condensing section	200 mm
Heat source temperature	170°C
Cooling liquid temperature (average)	68°C
Operating temperature	120 °C
Incline angle relative to horizontal	20°
Liquid fill level	425mm
Pipe material/ thickness	Copper, 0.376mm
Wick structure	Copper, screen, 2 wraps, 150 mesh count, 0.06mm wire diameter, 0.109mm×0.109mm aperture size, 42% open area.
Heat conduction/convection medium (evaporation section)	Still air
Heat conduction/convection medium (condensation section)	Circulated water
Working fluid	Water
Heat output	132 W
Maximum heat transport capacity	314W

Table 2. Energy balance and performance test data for the wicked heat pipe

Test No.	1	2	3
Items			
Ambient temperature,°C	23.60	23.46	23.50
HP evaporator temperature 1,°C	128.43	129.78	107.32
HP evaporator temperature 2, °C	137.03	138.22	114.56
HP evaporator temperature 3, °C	138.92	139.97	114.80
HP evaporator temperature 4, °C	138.64	139.99	116.90
Mean HP evaporator temperature, °C	135.76	136.99	113.39
Insulation layer temperature at HP evaporator, °C	64.11	64.36	55.81
HP adiabatic section temperature, °C	121.16	122.57	101.08
HP condenser temperature 1, °C	112.17	113.82	94.18
HP condenser temperature 2, °C	110.75	111.82	92.46
HP condenser temperature 3, °C	110.62	111.30	91.91
Mean HP condenser temperature, °C	111.18	112.31	92.85
Insulation layer temperature at HP condenser, °C	51.89	52.78	45.09
HP ΔT between evaporator and condenser, °C	24.57	24.68	20.54
Inlet temperature of cooling water, °C	39.80	41.39	36.55
Outlet temperature of cooling water, °C	95.34	95.53	78.38
Heater temperature, °C	175.8	173.2	150.4
Flow rate, CCM	35	35	35
Heat power, W	171.43	171.43	133.52
Estimated Heat loss, W	33.76	34.19	26.77
Power loss by water cooling, W	135.4	132.0	102.0

	4	5	3
Energy balance error, %	1.31	3.03	3.54

References

1. Faghri, A. (1995) Heat Pipe Science and Technology, Taylor & Francis, Washington, DC, pp. 11-110.
2. Collier, J. C., Convective Boiling and Condensation, McGraw-Hill, New York, 1981.
3. Colwell, G. T. and Chang, W. S., Measurement of the Transient Behavior of a Capillary Structure under Heavy Thermal Loading. International Journal of Heat and Mass Transfer, 1984, 27, 541-551.
4. Attili Basem S. (1994) Numerical study of the vapour flow characteristics of a slender cylindrical heat pipe. Energy Convers. Mgmt Vol. 35, No. 11, pp. 999-1008.
5. Lin Song, Hybrid CHP system, HP manufacture and performance tests, Internal report to project coordinator, March 2002.

Figure 1. View of the test rig

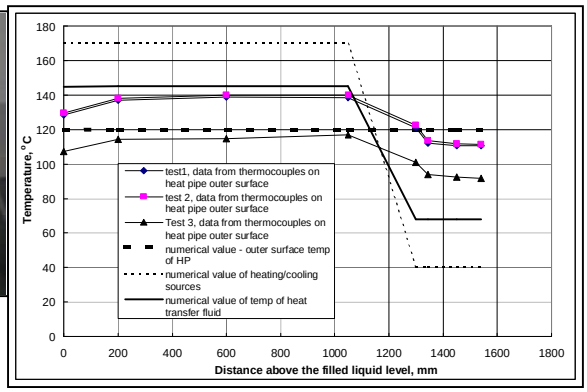

Figure 2. Comparison of numerical and experimental results for temperature profile